X Ray Diffraction with a Double Hot-Plate Laser-Heated Diamond Cell

Ho-kwang Mao, Guoyin Shen,[1] and Russell J. Hemley

Geophysical Laboratory and Center for High Pressure Research, Carnegie Institution of Washington, Washington, D. C.

Thomas S. Duffy[2]

Consortium for Advanced Radiation Sources, The University of Chicago, Chicago, IL

The laser-heated diamond cell has been improved with the integration of in-situ X ray microprobe and double hot-plate heating techniques. A multimode YAG laser provides a flat-top power distribution at the focal spot. A hot-plate configuration is created where the heat generation and temperature measurement are concentrated at the planar interface of an opaque sample and transparent medium. The heating laser is split into two beams that pass through the opposed diamond anvils to heat the sample simultaneously from both sides. The temperatures of the two sides are measured separately with an imaging spectrograph and CCD and equalized by controlling the ratio of beam splitting. The axial temperature gradient in the sample layer is eliminated within the cavity of the two parallel hot plates. Uniform temperatures of 3000 (± 20) K have been achieved in high-pressure samples of 15-μm diameter × 10-μm thickness. X ray microprobe beam sizes down to 3.5 × 7 μm (i.e., significantly smaller than the laser heating spot) were used for in situ characterization of the samples under high *P-T* conditions. The technique has been used to study phase relations and melting of iron.

1. INTRODUCTION

Accurate determination of phase diagrams and *P-V-T* equations of state of materials at conditions of planetary deep interiors has been a long-sought goal of experimental geophysics [*Mao and Hemley*, 1996]. Although the conditions at the Earth's core can be achieved with a laser-heated diamond cell [*Boehler*, 1996; *Jeanloz and Kavner*, 1996; *Jephcoat and Besedin*, 1996; *Lazor and Saxena*, 1996] the results are often perceived as ambiguous or represent disequilibrium conditions. While the samples absorbing the laser beam are heated to thousands of degrees, other parts of the high-pressure apparatus remain cool and undisturbed [*Bodea and Jeanloz*, 1989]. The large temperature gradient and the small heating spot are essential for achieving extreme conditions, but they are detrimental to defining precise temperatures. Thermal pressure generated by localized heating adds large uncertainty and inhomogeneity to the pressure, which is normally measured in a calibrant in an unheated region adjacent to the sample. Temperature gradients also cause non-equilibrium chemical diffusion and differentiation in an originally homogeneous sample [*Campbell et al.*, 1992].

[1]Present Address: Consortium for Advanced Radiation Sources, The University of Chicago, 5640 S. Ellis Ave., Chicago, IL 60637

[2]Present Address: Department of Geosciences, Princeton University, Princeton, NJ 08544

Properties of Earth and Planetary Materials
at High Pressure and Temperature
Geophysical Monograph 101

Characterization of laser-heated diamond-cell samples is typically carried out after quenching to ambient temperature at high pressures [*Bassett and Ming*, 1972; *Liu*, 1975; *Mao et al.*, 1977]. Measurement techniques used with in situ studies at high *P-T* often suffer from non-unique interpretations. For example, melting of iron has been determined on the basis of visual criteria or temperature-laser power correlation [*Williams and Jeanloz*, 1991; *Boehler*, 1993; *Saxena et al.*, 1993; *Jeanloz and Kavner*, 1996]. In principle, in situ X ray diffraction during laser heating provides definitive information on crystal structure and density. However, only a handful of examples have been reported to date and these are considered largely reconnaissance studies [*Boehler et al.*, 1990; *Meade et al.*, 1995; *Saxena et al.*, 1995; *Serghiou et al.*, 1995; *Yoo et al.*, 1995; *Fiquet et al.*, 1996]. X ray diffraction studies could be improved by maximizing the heating spot size, X ray intensity, spatial resolution, and diffraction accuracy, and minimizing the *P* gradients, *T* gradients, *T* fluctuations, sample differentiation, and X ray sampling time. Because of the interdependence of these factors, an integrated approach for constraining the overall experimental uncertainty is essential.

2. TEMPERATURE, PRESSURE, AND SAMPLE

2.1. *Double Hot Plates*

During laser heating, a steady-state temperature distribution is reached in diamond cell samples as heat is generated by absorption of the laser and dissipated by flowing down temperature gradient. Severe temperature gradients in the sample exist along the path of the laser beam (i.e., axially) [*Manga and Jeanloz*, 1996]. The diamond anvils, with their characteristic high thermal conductivity, dissipate the heat efficiently and constrain the low-temperature boundary condition. In a semi-transparent dielectric sample (absorbance $A < 1$), the laser is partially absorbed as it passes through the sample, resulting in a peak temperature near the middle and lower temperatures on both sides of the sample. For an opaque sample ($A >> 1$), the laser beam is blocked and absorbed at the sample-medium interface. Heat is generated only at the interface and is conducted to the opposite side of the sample, resulting in a monotonically decreasing temperature through the thickness of the sample. The axial temperature difference in the sample can be reduced by minimizing the sample thickness. However, a very thin sample is undesirable because it also reduces the signal for in situ measurement.

In the present study, the axial temperature gradient in the sample is eliminated by adopting a "double hot-plate" configuration (Figure 1) [*Shen et al.*, 1996]. An opaque sample is sandwiched between two layers of transparent media. Two coaxial but opposing laser beams are focused on opposite sides of the sample. The power of the two beams is adjusted so that both sample-medium interfaces are heated to the same temperature. Acting like planar heat sources, the two "hot plates" eliminate the axial temperature gradient in the sample between the plates and leave a steep gradient in the transparent media outside. The double-side laser-heating geometry, although not necessarily in the hot-plate configuration, has been previously reported by *R. Boehler* [1993, personal communication].

2.2. *Radial Temperature Gradient*

The radial temperature distribution across a heated spot corresponds closely to the power distribution of the laser beam, being only slightly modified by radial heat conduction. The commonly used TEM_{00} laser mode has a small beam diameter and low divergence that can be focused to generate a Gaussian-like power distribution; this is undesirable because the spot size at the peak temperature is a very small portion of the Gaussian. For example, in a conventional experiment of heating an iron sample at 50 GPa to 3000 K by a 15W TEM_{00} YAG laser, the diameter of the spot at 95% maximum temperature (2700 K) is only ~5 μm, but that at 50% maximum (1500 K) is 20 μm. Enlarging the area in the sample at the peak

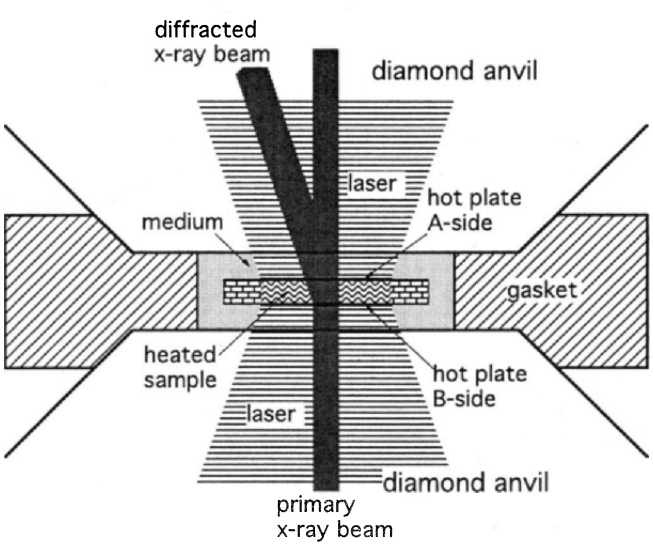

Figure 1. Double hot plate geometry.

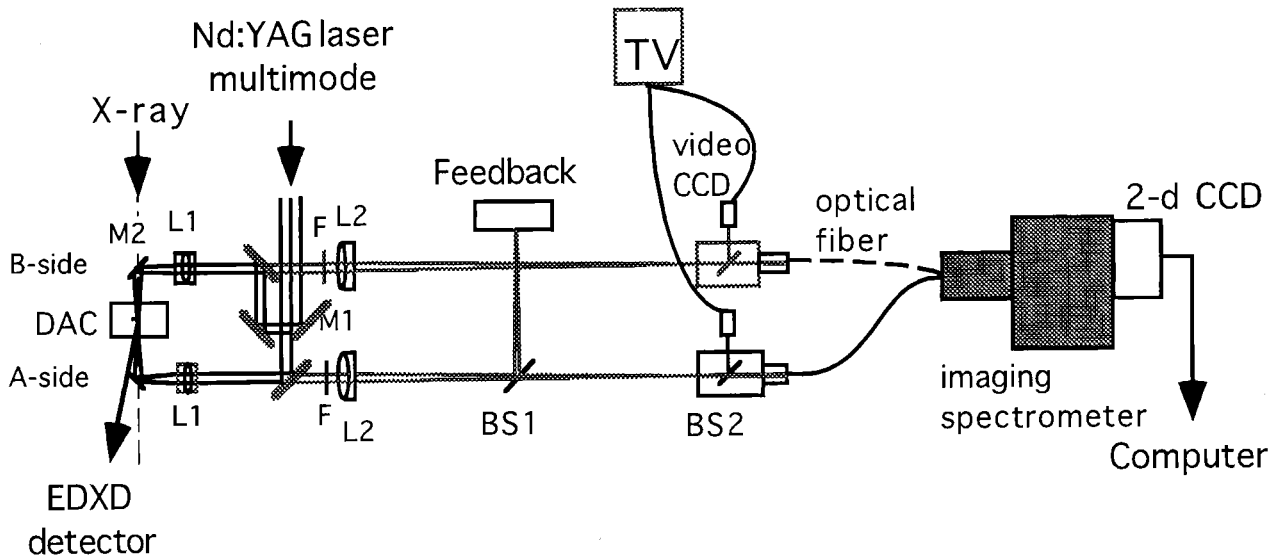

Figure 2. Schematic of the optical system for simultaneous double hot-plate laser-heating and X ray diffraction.

temperature requires increasing the laser power and altering the beam profile to a flat-top (i.e., boxcar) shape. Typical TEM_{00} YAG (or YLF) lasers are limited to ~30 W. The CO_2 laser has been used to deliver 100-200 W and to provide a larger heating spot [*Boehler and Chopelas*, 1992; *Yagi and Susaki*, 1992].

We explored several methods to achieve a flat-top power distribution with high peak temperature. (1) We used a 100-W multimode cw YAG laser which naturally provides a favorable flat-top power distribution. The multimode laser has sufficient power to be split into two beams for double hot-plate heating. Experimental results obtained by this method are presented in this paper. (2) We tested focusing the laser beam onto an optical fiber, which scrambles the mode shape and provides an output with a uniform power distribution across the fiber diameter. The output is refocused into the diamond cell to produce a hot spot with a flat-top power distribution (full-width-95%-maximum of 50 μm). (3) We have also directed the output of two separate YAG lasers (one adjusted for TEM_{00}, the other TEM_{01}) onto each side of the hot plates, which also doubles the total power.

2.3. *Coaxial Optical System*

A schematic diagram of the optical system is shown in Figure 2. A multimode Nd:YAG laser beam is split into two paths: A, reflected from mirror M1, and B, which bypassing M1. The two beams are focused by lens L1 and reflected by beryllium mirrors M2, which reflect visible-to-infrared radiation and transmit incident and diffracted high-energy X radiation. Optical images are monitored from both sides (A and B) of the diamond cell by 2 video CCD (TV) and are adjusted for coaxial alignment of the two heating spots to a spatial accuracy of ±2 μm. Thermal radiation from both sides is focused into optical fibers and dispersed by an imaging spectrometer onto a two-dimensional CCD for temperature measurements. Temperatures of A and B sides are equalized by adjusting the M1 mirror position, which controls the ratio of the laser beam splitting. The laser beams, thermal radiation, and optical images are all focused to the diamond surface with normal incidence to minimize astigmatism.

2.4. *Temperature Determination, Stabilization, and Distribution*

The temperature of the laser-heated sample is determined from its incandescence spectrum. For a transparent or semi-transparent sample, the spectrum is the summation of emission from the sample and media through the entire axial temperature gradient. Corrections and assumptions are applied to deconvolute the peak temperature from the combined spectra [*Boehler*, 1996; *Jeanloz and Kavner*, 1996]. The uncertainty is minimized in the present configuration with an opaque sample (absorbance $A \gg 1$ at 400–900 nm) and transparent medium ($A < 0.01$ at 400–900 nm). The transparent medium, in which the steep temperature gradient is located, has a very low emissivity. Its thermal emission is

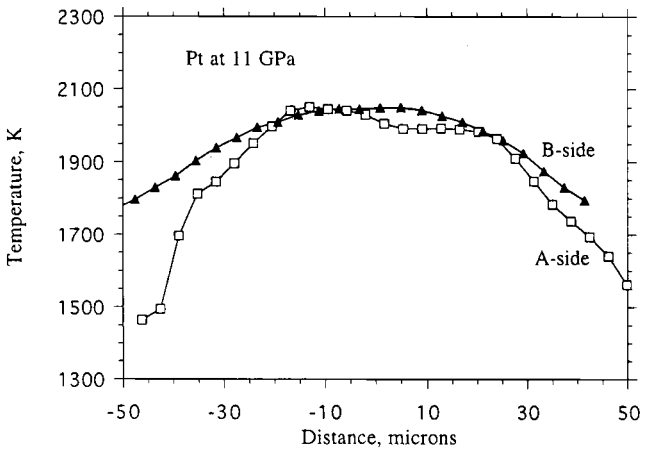

Figure 3. Temperature distribution of A and B sides of a Pt foil at 11 GPa.

insignificant in comparison to that of the highly-emissive, opaque hot plates, and has little effect on the temperature measurement at the opaque sample-medium interface. The spectra are collected with an imaging spectrograph and area (CCD) detector. The radial temperature distribution is mapped with optical microprobes of 3-μm spatial resolution. Figure 3 shows a representative measurement at 11 GPa and 2000 K in which the temperature is uniform to within ±0.5% in a 15-μm area, or ±3% within a 50-μm area, on both sides A and B.

Temperature varies with the fluctuation in laser power and the change of sample-medium absorption characteristics. Variations are reduced with feedback control of the heating power [*Boehler and Chopelas*, 1991]. However, the use of a polarizer to attenuate TEM_{00} laser power [*Heinz et al.*, 1991] is ineffective for the multimode laser used in the present system. We regulate the temperature by an electronic feedback circuit monitoring thermal radiation from the sample and adjusting the electrical power of the laser (Figure 2). The precision of temperature stabilization depends upon the temperature, pressure, and heating time. Figure 4 shows temperatures stabilized to ±0.5% at 2000 K and 11 GPa for 300 s and to ±3% at 2950 K and 30 GPa for 550 s, both are sufficient time for X ray diffraction studies.

2.5. *Symmetrical Diamond Cell*

In the Mao-Bell type of piston-cylinder diamond cell commonly used for experiments in the 100-GPa pressure range [*Mao et al.*, 1994], the sample is located near the cylinder end. The asymmetric arrangement severely restricts the optical access on the piston side and is unsuitable for the double hot-plate configuration. A new type of diamond cell with symmetrical access has been designed and used up to 220 GPa at room temperature. In the new device (Figure 5), the piston-cylinder is sufficiently long (length : diameter = 1) for mechanical stability at ultrahigh pressures. The sample is at a symmetrical position with 60° conical openings on both piston and cylinder sides for double hot-plate heating and measurements.

2.6. *Samples and media*

Opaque materials are studied with the double laser heating of the sample sandwiched between two layers of transparent material. The thickness of medium layers affects the heat dissipation and temperature distribution. Plastic flow of an initially uniform medium may result in an uneven thickness that reduces the size of the uniform-temperature region on increasing pressures. In Figure 3, for example, the 3% variation in temperature of sides A and B over the 50-μm area is due to a kink in the distribution caused by uneven thickness of the medium on side A. We have experimented with Pt, Re, W, Ir, Os, Fe, Si, Al, B, Be, FeO, and FeS as the opaque sample and sapphire, MgO, NaCl, LiF, Ne, and Ar as the transparent media. Because chemical reactivity between medium and sample may change at high pressures and temperatures, it is prudent to conduct redundant studies of the same sample with different media to test their chemical compatibility.

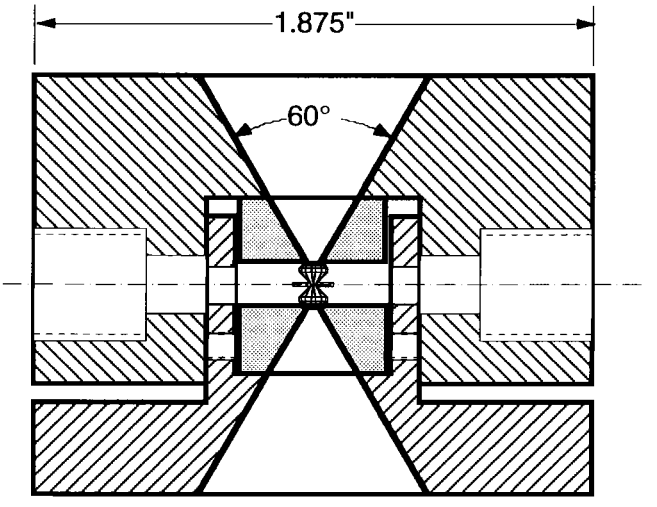

Figure 4. Temporal temperature variations with the feedback stabilizer at 11 GPa - 2000 K and 30 GPa - 3000 K.

For transparent samples (e.g., $MgSiO_3$) which do not naturally absorb the laser and have a black-body emission spectrum, we have experimented with three methods for fabricating the opaque layer: (1) by mixing the sample with metallic powders, (2) by sputtering with a metallic coating, or (3) by sandwiching between thin metallic foils. The third method, although requiring complicated 5-layer fabrication (medium-metal-sample-metal-medium), more reliably produces an opaque interface for the double hot-plate configuration.

3. X RAY DIFFRACTION MICROPROBE

3.1. *X ray Microbeam Size*

A glancing angle mirror system [*Yang et al.*, 1995] has been developed for focusing polychromatic synchrotron X ray beams to a microscopic spot size. The system consists of two bent Kirkpatrick-Baez (K-B) mirrors made of platinum-coated glass plates that reflect 90% of incident X ray photons up to the cut-off energy of 70 keV at 1 mrad glancing angle. In trial experiments, the synchrotron X ray beam was first focused in the vertical plane by the first mirror (260 mm focal distance) and in the horizontal plane by the second mirror (150 mm focal distance). The mirrors intercepted a 50-μm (h) × 70-μm (v) beam and focused it to 7-μm (h) × 3.5-μm (v) (Figure 6), resulting in a hundred fold increase in unit-area intensity. In routine experiments, the beam size was always ≤ 10 × 10 μm. The size of the focused X ray beam at the sample is therefore significantly smaller than the double laser-heated spot. With improved spatial and temporal resolution, energy dispersive X ray diffraction (EDXD) from diamond cell samples can be obtained at comparatively uniform and constant *P-T* (±0.5% in *T*)

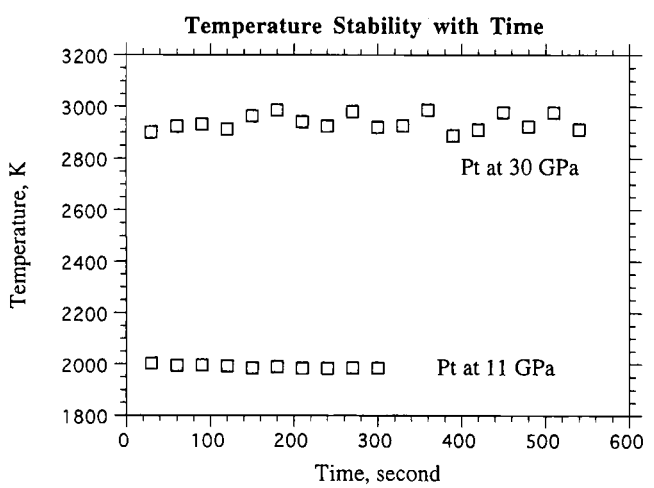

Figure 5. Symmetrical diamond cell for double-sided laser heating.

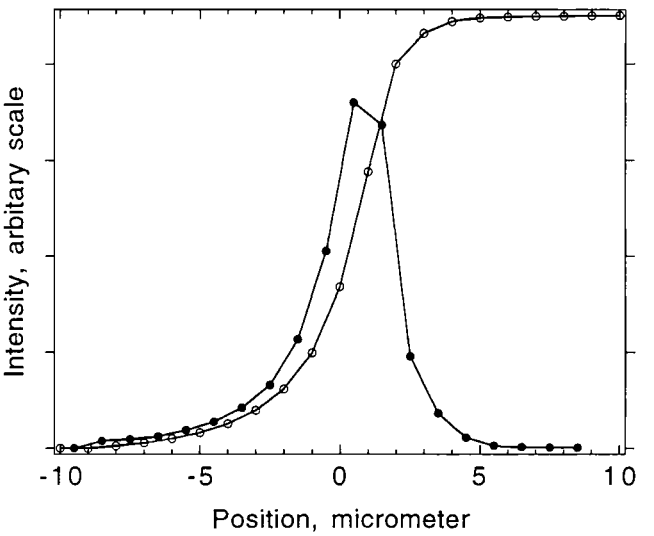

Figure 6. Step-scanning a sharp edge (for blocking the beam) across the focused X ray microbeam in the vertical direction. S-shaped curve (opened circles) shows the intensity measurement. The FWHM of the derivation (bell-shaped curve and solid circles) gives an approximate measure of the focused beam size.

3.2. *X ray Microbeam Position*

The position of the X ray microbeam must be coordinated with the laser-heating spot. For coarse alignment, a two-dimensional step scan of the diamond cell across the X ray microbeam provides a transmission radiographic image showing the details of the diamond culet, gasket hole, and sample shape. The heating laser spot and the details of the sample chamber are also viewed with an optical microscope and a video camera. The X ray image is coordinated with the optical image to ±5 μm accuracy. Finer alignment to ±2 μm accuracy is achieved by tuning the X ray beam to maximize the fluorescence of a 5-μm grain of gold marker in the sample chamber. With its position known, the X ray microbeam can be placed precisely at the center of laser spot where the temperature is maximum, and gradient is minimum.

3.3. *Preferred Orientation and Coarse Crystallinity*

The extremely small and intense X ray beam ensures *P-T* uniformity within the probed region, but greatly reduces the number of crystallites sampled. Crystal growth within the laser-heated zone further compounds the problem of

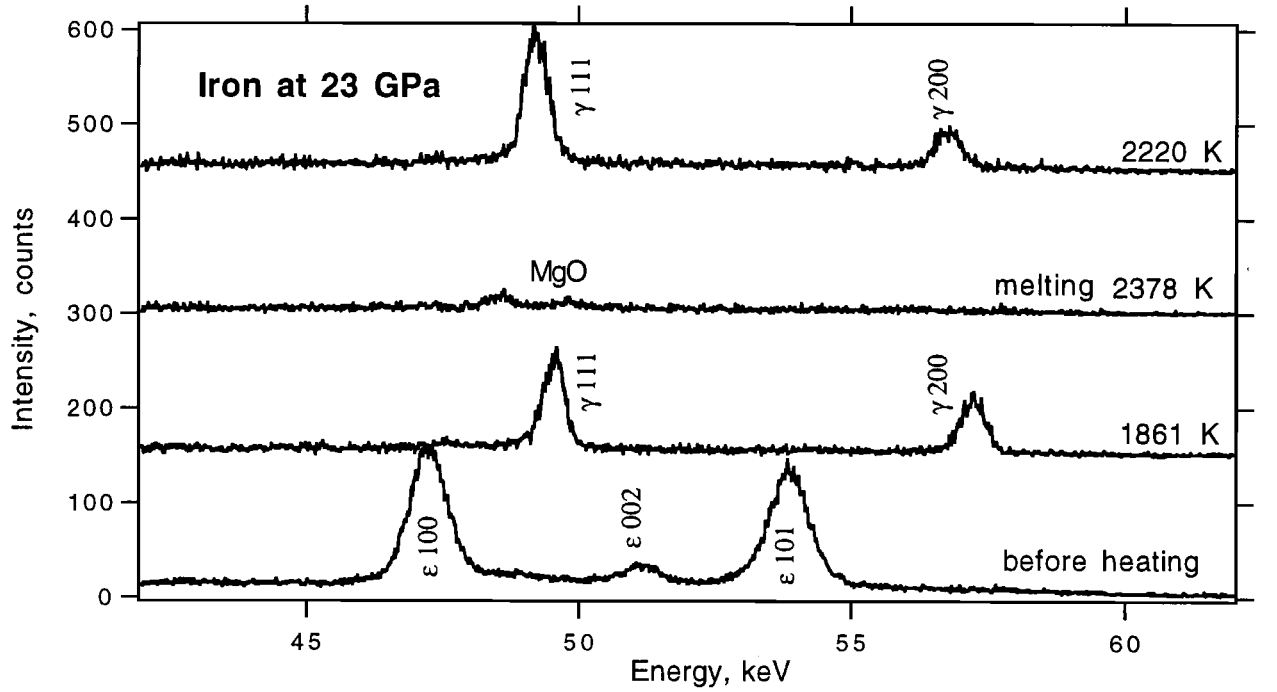

Figure 7. EDXD pattern of iron at 23 GPa as a function of the heating cycle; $2\theta = 7.166°$; $E(\text{keV})d(\text{Å}) = 99.198$.

preferred orientation and coarse crystallinity; this can lead to unreliable peak intensities in the polycrystalline EDXD pattern and even missing diffraction peaks. We have resolved this problem by rotating the diamond cell around its axis; the entire 2θ cone is sampled and averaged at each revolution (typically 50–100 rpm). The diamond cell is centered in the rotation stage (±3 μm) so that the laser beam, X ray beam, and diamond axis are all coaxial with the rotation stage. Consequently, the heating spot position and the sample temperature is constant during rotation. The rotation is crucial for high *P-T* melting studies where recrystallization is rapid near the liquidus.

4. EXAMPLE—PHASE TRANSITIONS AND MELTING OF IRON

Understanding phase transitions and melting of iron is central to models of the Earth's core, and thus the high *P-T* behavior of iron has been the focus of numerous static compression studies. However, the reported melting curves spread over a wide temperature range as a result of the aforementioned experimental difficulties [*Boehler*, 1996; *Jeanloz and Kavner*, 1996; *Jephcoat and Besedin*, 1996; *Lazor and Saxena*, 1996]. We applied the present technique to study iron under high *P-T* conditions. Thin iron foils sandwiched between Al_2O_3, MgO, or NaCl were compressed in the new type of diamond cell and heated with the double hot-plate method and a multimode YAG laser. X ray diffraction was performed at the superconducting wiggler beamline X17B1 at the National Synchrotron Light Source.

Representative diffraction patterns are shown in Figure 7. At 23 GPa and room temperature, iron crystallizes in hexagonal-close-packed (hcp) structure (ε-Fe). As the temperature was raised to 1861 (±50) K, the hcp diffraction lines disappeared completely, and new lines corresponding to the face-centered-cubic (fcc) phase (γ-Fe) appeared. Above 2378 (±50) K, the diffraction peaks of γ-Fe disappeared, and MgO diffraction peaks, which are much weaker that of crystalline iron, became observable. Iron peaks reappeared when temperature was lowered to 2220 (±50) K, bracketing the melting temperature. The completeness of the transition indicates that the X ray beam sampled a comparatively uniform *P-T* region, a major improvement over previous experiments [e.g., *Yoo et al.*, 1995]. Melt and crystalline phases of iron observed in distinct *P-T* regions are shown in Figure 8. Although a systematic study is needed to complete the determination of the phase diagram, the present data indicate that the melting curve is lower than that of *Williams and Jeanloz* [1991] but higher than that of *Boehler et al.* [1990], *Shen et al.* [1993], and *Saxena et al.* [1993]. The liquidus phase

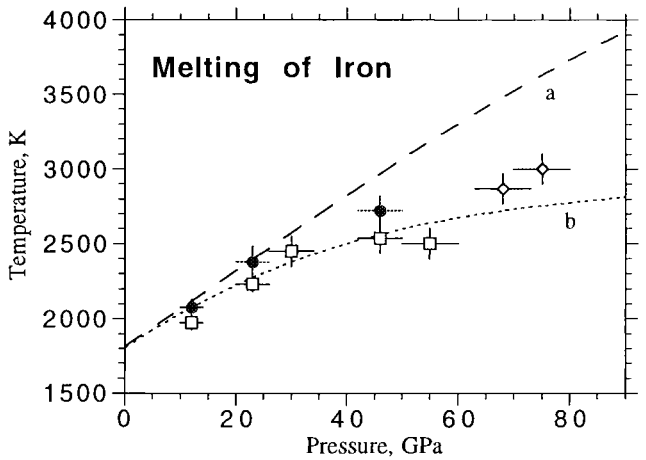

Figure 8. Results of high-*P-T* X ray diffraction of iron; open square, fcc pattern; open diamond, hcp pattern; solid circle, no diffraction peaks; dashed line (a), melting curve from *Williams and Jeanloz* [1991]; dotted line (b), melting curve taken from the combined studies of *Boehler et al.* [1990], *Shen et al.* [1993], and *Saxena et al.* [1993].

changes from γ at 55 GPa to ε at 68 GPa, resulting in a γ-ε-liquid triple point near 60 GPa [*Yoo et al.*, 1995]. The new data demonstrate the feasibility of performing high-precision phase equilibria studies and the prospect for measurements such as equations of state, at the *P-T* conditions of the deep mantle and core with the double hot-plate laser-heated diamond cell.

Acknowledgments. This work is supported by the National Science Foundation. We thank the National Synchrotron Light Source for beam time at X17B1.

REFERENCES

Bassett, W. A., and L. C. Ming, Disproportionation of Fe_2SiO_4 to $2FeO + SiO_2$ at pressure up to 250 kilobars and temperatures up to 3000°C, *Phys. Earth Planet. Interiors, 6*, 154-160, 1972.

Bodea, S., and R. Jeanloz, Model calculations of the temperature distribution in the laser-heated diamond cell., *J. Appl. Phys., 65*, 4688-4692, 1989.

Boehler, R., Temperatures in the Earth's core from melting-point measurements of iron at high static pressures, *Nature, 363*, 534-536, 1993.

Boehler, R., Melting of mantle and core materials at very high pressures, *Phil. Trans. R. Soc. Lond. A, 354*, 1265-1278, 1996.

Boehler, R., and A. Chopelas, A new approach to laser heating in high pressure mineral physics, *Geophys. Res. Lett., 18*, 1147-1150, 1991.

Boehler, R., and A. Chopelas, Phase transition in a 500 kbar - 3000 K gas apparatus, *High-Pressure Research: Application to Earth and Planetary Sciences*, edited by Y. Syono and M. H. Manghnani, pp. 55-60, Terra Scientific Publishing Co., Tokyo/AGU, Washington, D. C. 1992.

Boehler, R., N. von Bargen, and A. Chopelas, Melting, thermal expansion, and phase transitions of iron at high pressures, *J. Geophys. Res., 95*, 21,731-21,736, 1990.

Campbell, A. J., D. L. Heinz, and A. M. Davis, Material transport in laser-heated diamond anvil cell melting experiments, *Geophys. Res. Lett., 19*, 1061-1064, 1992.

Fiquet, G., D. Andrault, J. P. Itié, P. Gillet, and P. Richet, X-ray diffraction in a laser-heating diamond-anvil cell, *Advanced Materials '96 - New Trends in High Pressure Research*, pp. 153-158, Nat. Inst. Res. Inorganic Mat., Tsukuba, Japan, 1996.

Heinz, D. L., J. S. Sweeney, and P. Miller, A laser heating system that stabilizes and controls the temperature: Diamond anvil cell applications, *Rev. Sci. Instrum., 62*, 1568-, 1991.

Jeanloz, R., and A. Kavner, Melting criteria and imaging spectroradiometry in laser heated diamond-cell experiments, *Phil. Trans. R. Soc. Lond. A, 354*, 1279-1305, 1996.

Jephcoat, A. P., and S. P. Besedin, Temperature measurement and melting determination in laser-heated diamond-anvil cells, *Phil. Trans. R. Soc. Lond. A, 354*, 1333-1360, 1996.

Lazor, P., and S. K. Saxena, Discussion comment on melting criteria and imaging spectroradiometry in laser-heated diamond-cell experiments (by R. Jeanloz & A. Kavner), *Phil. Trans. R. Soc. Lond. A, 354*, 1307 -1313, 1996.

Liu, L. G., Post-oxide phases of olivine and pyroxene and mineralogy of the mantle, *Nature, 258*, 510-512, 1975.

Manga, M., and R. Jeanloz, Axial temperature gradients in dielectric samples in the laser-heated diamond cell, *Geophys. Res. Lett., 23*, 1845-1848, 1996.

Mao, H. K., and R. J. Hemley, Experimental studies of Earth deep interior: Accuracy and versatility of diamond cells, *Phil. Trans. R. Soc. Lond. A, 354*, 1-18, 1996.

Mao, H. K., R. J. Hemley, and A. L. Mao, Recent design of ultrahigh-pressure diamond cell, *High Pressure Science and Technology --1993*, vol. 2, edited by S. C. Schmidt, J. W. Shaner, G. A. Samara and M. Ross, pp. 1613-1616, AIP Press, New York, 1994.

Mao, H. K., T. Yagi, and P. M. Bell, Mineralogy of the earth's deep mantle: quenching experiments on mineral compositions at high pressure and temperature, *Carnegie Inst. Washington Yearb., 76*, 502-504, 1977.

Meade, C., H. K. Mao and J. Hu, High-temperature phase transition and dissociation of $(Mg,Fe)SiO_3$ perovskite at lower mantle pressures, *Science, 268*, 1743-1745, 1995.

Saxena, S. K., L. S. Dubrovinsky, P. Haggkvist, Y. Cerenius, G. Shen and H. K. Mao, Synchrotron X-ray study of iron at high pressure and temperature, *Science, 269*, 1703-1704, 1995.

Saxena, S. K., G. Shen, and P. Lazor, Experimental evidence for a new iron phase and implications for Earth's core, *Science, 260*, 1312-1314, 1993.

Serghiou, G., A. Zerr, L. Chudinovskikh, and R. Boehler, The coesite-stishovite transition in a laser-heated diamond cell, *Geophys. Res. Lett., 22*, 441-444, 1995.

Shen, G., P. Lazor, and S. K. Saxena, Melting of wüstite and iron up to pressures of 600 kbar, *Phys. Chem. Mineral., 20*, 91-96, 1993.

Shen, G., H. K. Mao, and R. J. Hemley, Laser-heating diamond-anvil cell technique: Double-sided heating with multimode Nd:YAG laser, *Advanced Materials '96 - New Trends in High Pressure Research*, pp. 149-152, Nat. Inst. Res. Inorganic Mat., Tsukuba, Japan, 1996.

Williams, Q., and R. Jeanloz, The high pressure melting curve of iron: A technical discussion, *J. Geophys. Res.*, *96*, 2171-2184, 1991.

Yagi, T., and J. Susaki, A laser heating system for diamond anvil using CO_2 laser, *High-Pressure Research: Application to Earth and Planetary Sciences*, edited by Y. Syono and M. H. Manghnani, pp. 51-54, Terra Scientific, Tokyo/AGU, Washington, D. C. 1992.

Yang, B. X., M. Rivers, W. Schildkamp, and P. J. Eng, GeoCARS microfocusing Kirkpatrick-Baez mirror bender development, *Rev. Sci. Instrum.*, *66*, 2278-2280, 1995.

Yoo, C. S., J. Akella, A. J. Campbell, H. K. Mao, and R. J. Hemley, Phase diagram of iron by in situ x-ray diffraction: implications for the Earth's core, *Science*, *270*, 1473-1475, 1995.

H. K. Mao, G. Shen, and R. J. Hemley, Geophysical Laboratory and Center for High Pressure Research, Carnegie Institution of Washington, 5251 Broad Branch Rd. NW, Washington, D. C. 20015

T. S. Duffy, Consortium for Advanced Radiation Sources, The University of Chicago, 5640 S. Ellis Ave., Chicago, IL 60637